Refined Crystal Structure and Mechanical Properties of Superhard BC_4N Crystal: First-Principles Calculations

Xiaoguang Luo,[†] Xiang-Feng Zhou,[‡] Zhongyuan Liu,[†] Julong He,[†] Bo Xu,[†] Dongli Yu,[†] Hui-Tian Wang,[‡] and Yongjun Tian*[,†]

State Key Laboratory of Metastable Materials Science and Technology, Yanshan University, Qinhuangdao 066004, China, and National Laboratory of Solid State Microstructures and Department of Physics, Nanjing University, Nanjing 210093, China

Received: February 20, 2008; Revised Manuscript Received: April 13, 2008

Synthesized cubic BC_4N with Vickers hardness 10% higher than that of cubic BC_2N exhibits a strange X-ray diffraction spectrum, assigned as a zinc-blende cubic structure. However, its crystal structure cannot be constructed with a zinc-blende structure as viewed from the stoichiometric formula. We found that this structure can be described by 3*C*-BC_4N in Ramsdell notation, with the space group of *P*3*m*1. First-principles calculations show that this so-called "cubic" BC_4N is a large gap insulator and has outstanding mechanical properties such as an ideal tensile strength of 77.1 GPa and a theoretical Vickers hardness of 84.3 GPa. The simulated Raman spectra of five 3*C*-BC_4N configurations show totally different features, providing a valid method to conclusively determine the atomic arrangement of cubic BC_4N.

Potential superhard crystals in the ternary boron carbon nitrogen (B−C−N) system have attracted a great deal of attention in seeking novel superhard crystals with hardness comparable to diamond since the prediction of superhard β-C_3N_4 crystal.[1] The ternary superhard B−C−N crystals are predicted to exhibit properties that are comparable or even superior to those of diamond and cubic boron nitride (*c*-BN), making them have a wide variety of potential applications in science and technology. Since superhard *c*-BC_2N (refs 2, 3) and *c*-BC_4N (ref 3) crystals were successfully synthesized by using diamond-anvil cell and multianvil press, many investigations based on first-principles calculations[4–11] have been carried out on the possible refined crystal structure, ideal strength, and Vickers hardness of *c*-BC_2N. Although experimentalists claimed that their in situ and ex situ synchrotron X-ray diffraction (XRD) data support the primary results of assigning both *c*-BC_2N (refs 2, 3) and *c*-BC_4N (ref 3) as zinc-blende (ZB) cubic structure, the theoretical results demonstrate that for *c*-BC_2N all of the proposed hypothetical structures that originated from ZB mismatch the experimental XRD and Raman data.[2,3,12] Thereby the refined crystal structure of *c*-BC_2N has become a heated argument. On the basis of the 16-atom supercell of diamond in first-principles calculations, very recently, we have successfully determined the exact atomic arrangement of *c*-BC_2N crystal by carefully comparing the simulated XRD and Raman spectra of the hypothetical structure with those measured for *c*-BC_2N. The determined structure named *t*-BC_2N (ref 13) has the tetragonal symmetry with the space group of *P*-421*m*, whose simulated XRD and Raman spectra as well as estimated theoretical Vickers hardness are in excellent agreement with the corresponding experimental results. For the synthesized *c*-BC_4N crystal, the reported experimental Vickers hardness is 10% higher than that for the synthesized *c*-BC_2N crystal;[3] however, its refined crystal structure is still unclear up to now. Determining the refined crystal structure and manifesting the mechanical properties of *c*-BC_4N is a very important and challenging task for a deep and comprehensive understanding of structural features and functional properties of stoichiometric crystals in the ternary B−C−N system.

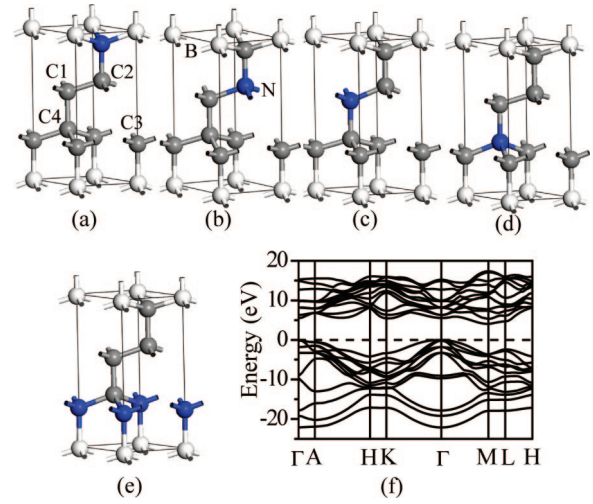

Figure 1. Crystal structures of (a) BC_4N-1, (b) BC_4N-2, (c) BC_4N-3, (d) BC_4N-4, and (e) BC_4N-5. Band structure (f) of BC_4N-1.

The experimental XRD result has suggested that the synthesized superhard *c*-BC_4N belongs to the ZB structure with the face-centered cubic unit cell of $a = 3.586$ Å.[3] Strictly speaking, there are eight atoms in the unit cell of the ZB structure. For the stoichiometric BC_4N, its unit cell consists of 6 or 12 atoms; in other words, it is impossible to construct *c*-BC_4N structures from the eight-atom ZB unit cell. If considering a supercell, theoretically, *c*-BC_4N cannot still belong to the ZB structure family according to its stoichiometric formula. Therefore, we have to seek another clue to configure the unit cell of *c*-BC_4N. On the basis of the experimental XRD result, of course, the considered structure should be similar or close to diamond or *c*-BN. As is well-known, diamond and *c*-BN can be considered

* To whom correspondence should be addressed. E-mail: fhcl@ysu.edu.cn.
† Yanshan University.
‡ Nanjing University.

10.1021/jp801530z CCC: $40.75
Published on Web 06/03/2008

TABLE 1: Equilibrium Lattice Parameters, Density (ρ), Total Energy (E_t), Formation Energy (E_f), Bulk Modulus (B), and Shear Modulus (G) for Five 3*C*-BC_4N Configurations, 3*C*-Diamond, and 3*C*-BN[a]

	BC_4N-1	BC_4N-2	BC_4N-3	BC_4N-4	BC_4N-5	3*C*-diamond	3*C*-BN	*c*-BC_4N (expt)
symmetry	*P*3*m*1	*P*3*m*1	*P*3*m*1	*P*3*m*1	*P*3*m*1	*Fd*-3*m*	*F*-43*m*	
a (Å)	2.507	2.544	2.545	2.544	2.540	2.493	2.539	2.535
c (Å)	6.196	6.192	6.205	6.202	6.179	6.107	6.218	6.211
c/*a*	2.472	2.434	2.439	2.438	2.433	2.450	2.449	2.450
ρ (g/cm^3)	3.588	3.487	3.477	3.481	3.506	3.641	3.562	3.498
E_t (eV/atom)	−162.07	−161.366	−161.431	−161.343	−161.51	−155.46	−175.70	
E_f (eV/atom)	0.137	0.841	0.776	0.864	0.697			
B (GPa)	418.8	387.5	389.0	377.3	371.3	447.1	383.8	
G (GPa)	521.3	300.2	162.3	73.0	285.6	546.4	406.5	

[a] The experimental density is from ref 3.

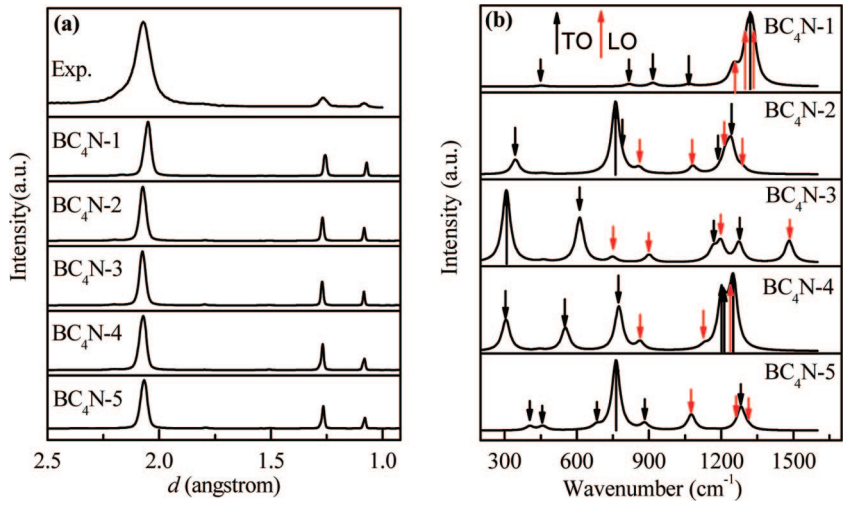

Figure 2. Simulated XRD spectra of five 3*C*-BC_4N configurations in comparison with the measured XRD spectrum of *c*-BC_4N (a), and the simulated Raman spectrum of five 3*C*-BC_4N (b).

as the same 3*C* structures as 3*C*-SiC in Ramsdell notation.[14] Therefore, the six-atom unit cell of the 3*C* structure is certainly a good candidate for the construction of dense BC_4N structures. Recently, a $BC_4N_{2\times1}$ superlattice has been predicted.[15] However, the unit cell of $BC_4N_{1\times1}$ translated from the $BC_4N_{2\times1}$ superlattice belonged to the 3*C* structure. In this Article, we report the 3*C* crystal structure of *c*-BC_4N matching the experimental XRD data. We investigate its electronic band structure, ideal tensile strength, and theoretical Vickers hardness, and we calculate the theoretical Raman spectra of different configurations in 3*C*-BC_4N. We found that the Raman spectra become an important criterion for accurately determining the atomic arrangement of *c*-BC_4N. In addition, the pressure-induced phase transition path from hexagonal BC_4N phase to *c*-BC_4N is also discussed.

The present calculations were performed with CASTEP code based on density functional theory.[16] The exchange-correlation function was treated by the local density approximation (LDA-CAPZ).[17,18] The norm-conserving pseudopotential[19] with cutoff energy of 770 eV and the *k* points of 12 × 12 × 4 according to the Monkhorst–Pack scheme[20] were used. The structure was relaxed by the Broyden–Fletcher–Goldfarb–Shanno methods.[21] The XRD patterns are simulated using the Reflex package in the MS Modeling. The calculation methods of ideal tensile strength are similar to the previous studies.[22,23] At each step, the fixed tensile strain was applied to the selected direction, and then the structural parameters were relaxed until the stress tensors orthogonal to the applied stress were less than 0.1 GPa. Therefore, a series of tensile stress corresponding to the incrementally applied tensile strains can be obtained. For the simulations of the Raman spectra, PWSCF code[24] was used within the framework of ab initio pseudopotential density functional perturbation theory.[25,26] A 80 Ry plane wave cutoff energy and 8 × 8 × 4 Monkhorst–Pack mesh of points in the Brillouin-zone were used. The detailed simulation procedure was described in ref 27.

Starting from the 3*C*-SiC structure, only five nonequivalent atomic configurations exist for BC_4N as shown in Figure 1. All of the configurations have the trigonal symmetry with the space group of *P*3*m*1. Both BC_4N-1 and BC_4N-5 exhibit a sandwich-like structure with an *ABCABC*... stacking sequence consisting of two C−C layers and one B−N layer along the *c*-axis direction. In the other three configurations, the B−N bonds are free. The relaxed structural parameters, total energy, and other considered properties of the five 3*C*-BC_4N configurations are summarized in Table 1, and the corresponding data of 3*C*-diamond, 3*C*-BN, and experimentally synthesized *c*-BC_4N in Ramsdell notation are also listed for comparison. In the BC_4N-1, the ratio of the number of C−C, B−N, B−C, and C−N bonds is 7:3:1:1, obeying the bond-counting rule,[28] so it has the lowest total energy among the five BC_4N configurations. The theoretical density of BC_4N-1 is 3.588 g/cm^3, which is between those of diamond and *c*-BN and slightly larger than the experimental value (3.498 g/cm^3) (ref 3) of *c*-BC_4N. As shown in Figure 1f, BC_4N-1 has an indirect band gap with the top of the valence band at the Γ point and the bottom of the conduction band at the *M* point. The band gap of 4.06 eV for BC_4N is less than those for diamond (E_g = 4.15 eV) and *c*-BN (E_g = 4.49 eV), while it is larger than those of the hypothetical ZB-BC_2N structures.[6] For the trigonal crystal with the classes of 3*m*, 32,

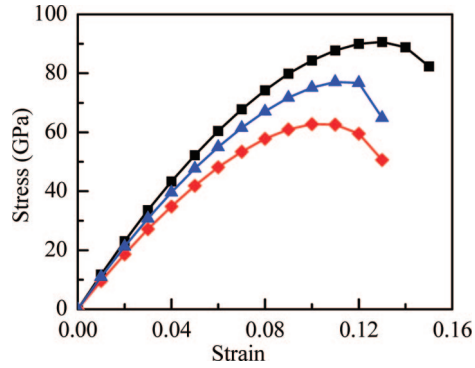

Figure 3. Calculated tensile stress−strain curves of BC_4N-1 (blue ▲), 3*C*-diamond (■), and 3*C*-BN (red ◆) along the *c* direction.

TABLE 2: Bond Parameters and the Calculated Vickers Hardness of Hypothetical BC_4N-1

bond type	n_i	d^{X-Y} (Å)	P^{X-Y}	N_e^{X-Y}	f_h^{X-Y}	f_i^{X-Y}	H_V^{X-Y}	H_V (GPa)
C1−C2	3	1.531	0.85	0.724	0.012	0.038	93.0	84.3
C2−N	1	1.500	0.46	0.694	0.083	0.161	82.2	
B−N	3	1.550	0.69	0.745	0.195	0.301	67.2	
B−C3	1	1.604	0.49	0.735	0.020	0.057	81.8	
C3−C4	3	1.532	0.84	0.723	0	0	97.0	
C1−C4	1	1.535	0.48	0.720	0.041	0.095	86.0	

and -3*m*,[29] its six independent elastic stiffness constants are given as c_{11}, c_{12}, c_{13}, c_{14}, c_{33}, and c_{44}. The complete set of these elastic constants for BC_4N-1 are listed as follows: $c_{11} = 1131.5$ GPa, $c_{12} = 75.8$ GPa, $c_{13} = 59.5$ GPa, $c_{14} = -6.7$ GPa, $c_{33} = 1116.9$ GPa, and $c_{44} = 508.5$ GPa. Clearly, the calculated elastic constants c_{ij} of BC_4N-1 satisfy the mechanical stability restrictions of $c_{11} - |c_{12}| > 0$, $(c_{11} + c_{12})c_{13} - 2(c_{13})^2 > 0$, and $(c_{11} - c_{12})c_{44} - 2(c_{14})^2 > 0$ for the trigonal structures.[30] Similar to the investigation in sp^3-bonded BC_2N, the formation energy of sp^3-bonded BC_4N can be defined as $E_f = E_{BC_4N} - (E_{3C\text{-BN}} + 2E_{3C\text{-diamond}})/3$. As shown in Table 1, all of the hypothetical 3*C*-BC_4N structures have positive formation energy, indicating that they are metastable and tend to separate into 3*C*-diamond and 3*C*-BN.

To determine the refined crystal structure of the synthesized *c*-BC_4N, we first simulate the XRD spectra. Figure 2a shows the comparison between the experimental XRD pattern of *c*-BC_4N and the simulated XRD patterns of five 3*C*-BC_4N configurations with the same grain size of 6 nm at the same wavelength of 0.4246 Å as those used in experiment.[3] Both measured and simulated XRD patterns exhibit three strong 111, 220, and 311 Bragg lines and one very weak 200 Bragg line in the *d*-spacing range from 1.0 to 2.5 Å. We found that all five simulated XRD patterns match that of *c*-BC_4N very well, implying that XRD is insensitive to the interchange of atom positions in B−C−N system. Because of the small difference of atomic number among B, N, and C atoms, in other words, it is difficult to conclusively determine the refined crystal structure of *c*-BC_4N from the XRD spectrum. Raman spectroscopy is sensitive to the atomic arrangement in a crystal even though component atoms are very adjacent in the Periodic Table of the elements; therefore, it becomes a very useful tool for the structural analysis of B−C−N crystal.[13] The simulated Raman spectra of the five 3*C*-BC_4N configurations are totally different in the strong peak position as shown in Figure 2b. For BC_4N-1, there are five visible transverse optical (TO) modes of 453.47, 816.83, 915.71, 1065.22, and 1325.28 cm^{-1}, and three longitudinal optical (LO) modes of 1250.28, 1306.44, and 1335.10 cm^{-1}. The strongest peak appears at about 1325 cm^{-1} (TO), and the second strongest peak at 1250 cm^{-1} (LO). For BC_4N-2 and BC_4N-5, their strongest peaks locate at about 761 cm^{-1} (TO), and their second strongest peaks at 1241 cm^{-1} (TO) and 1266 cm^{-1} (TO), respectively. For BC_4N-3 and BC_4N-4, their strongest peaks appear at 307 cm^{-1} (TO) and 1250 cm^{-1} (TO). Interestingly, the strongest Raman peak at 1325.28 cm^{-1} for BC_4N-1 almost overlaps the experimental Raman peak at 1325.7 cm^{-1} for the experimentally synthesized *c*-BC_2N.[12] The only difference between the Raman spectra of BC_4N-1 and *c*-BC_2N is that there is the second strong peak at 1250 cm^{-1} for BC_4N-1, which can be used to experimentally distinguish *c*-BC_4N from *c*-BC_2N. For the five configurations of BC_4N, obviously, their XRD spectra do not show much difference, while their Raman spectra exhibit very different features. Therefore, the simultaneous measurements of the XRD and Raman spectra are required for determining the atomic arrangement of a B−C−N crystal.

In the view of total energy or formation energy, BC_4N-1 can be assigned to *c*-BC_4N, which needs the further confirmation from the measurement of Raman spectrum as discussed above. Next, we will calculate the mechanical properties of BC_4N-1. The calculated bulk and shear moduli of BC_4N-1 are 418.8 and 521.3 GPa, respectively; both are very close to those of diamond and in good agreement with the values calculated by Vegard's law. Previous investigations have shown that the weakest tensile direction for diamond or *c*-BN is ⟨111⟩.[31] BC_4N-1 has the atomic positions similar to those of diamond; thus its weakest tensile direction should be along the *c*-axis in Ramsdell notation, corresponding to ⟨111⟩ in diamond. Therefore, here we calculate only the tensile stress as a function of the strain for 3*C*-diamond, 3*C*-BN, and BC_4N-1. As shown in Figure 3, the calculated ideal tensile strength of BC_4N-1 is 77.1 GPa, in agreement with the 79.3 GPa of $BC_4N_{2\times1}$ superlattice[15] but obviously larger than 60 GPa of *c*-BN and 68.4 GPa of $BC_2N_{1\times1}$ superlattices.[10] Because BC_4N-1 is a semiconducting polar covalent compound, its theoretical Vickers hardness can be estimated by using our microscopic model of hardness.[32] There are six types of chemical bonds in BC_4N-1 as shown in

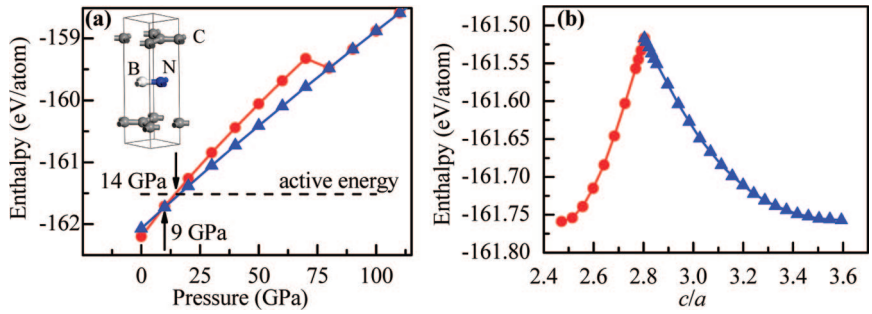

Figure 4. Enthalpy–pressure (a) and enthalpy–parameter *c*/*a* (b) relations of BC_4N-1 (blue ▲) and *h*-BC_4N-1 (red ●).

Table 2. According to our microscopic model of hardness,[32,33] the theoretical Vickers hardness of BC_4N-1 can be calculated as $H_V = [(H_V^{C1-C2})^{n_1}(H_V^{C2-N})^{n_2}(H_V^{B-N})^{n_3}(H_V^{B-C3})^{n_4}(H_V^{C3-C4})^{n_5}(H_V^{C1-C4})^{n_6}]^{1/n_1+n_2+n_3+n_4+n_5+n_6}$, where $H_V^{X-Y} = 350(N_e^{X-Y})^{2/3}e^{-1.191f_i^{X-Y}}/(d^{X-Y})^{2.5}$ is the hardness of the hypothetical binary compound composed of the X–Y bond, n_i ($i = 1-6$) is the number of the corresponding chemical bond, $N_e^{X-Y}$is the valence electron densities of the hypothetical compounds composed of the X–Y bond, and d^{X-Y} is the length of the X–Y bond. According to our generalized ionicity scale,[33] f_i^{X-Y} is the Phillips ionicity of the X–Y bond and can be calculated with $f_i^{X-Y} = (f_h^{X-Y})^{0.735} = [1 - \exp(-|P_c - P^{X-Y}|/P^{X-Y})]^{0.735}$, where f_h^{X-Y} is the new ionicity scale of the X–Y bond based on bond overlap population, P^{X-Y} is the overlap population of the X–Y bond, and P_c is the overlap population of the bond in a pure covalent crystal containing the same type of chemical bond. Here, we select the bond population in a pure covalent crystal of 3*C* diamond as P_c values. Two P_c values of 0.84 and 0.50 are obtained for the bond in bulked *a*–*b* plane and the bond along the *c*-axis, respectively. The calculated theoretical Vickers hardness of BC_4N-1 is 84.3 GPa, 10% larger than that (75.3 GPa) of the recently proposed hypothetical *t*-BC_2N of *c*-BC_2N.[13] This result is in good agreement with the experimental result for *c*-BC_4N.[3]

Similar to the relationship between 3*C*-diamond and 3*R*-graphite, the hypothetical graphite-like BC_4N (*h*-BC_4N) also has five corresponding configurations. As shown in the inset of Figure 4a, *h*-BC_4N with the lowest total energy, named as *h*-BC_4N-1, maintains the standard layered structure similar to *h*-BC_2N-F of hexagonal BC_2N.[34] *h*-BC_4N-1 has the same $P3m1$ symmetry as BC_4N-1. Therefore, we can calculate the pressure-induced phase transition from *h*-BC_4N-1 to BC_4N-1 with symmetry constraints. At zero pressure, *h*-BC_4N-1 is more stable than BC_4N-1. With the increase of pressure, the enthalpy of *h*-BC_4N-1 is equal to that of BC_4N-1 at the pressure of 9 GPa. However, the direct phase transition from *h*-BC_4N-1 to BC_4N-1 would not occur due to the existing energy barrier between the two phases. The curves of enthalpy versus *c*/*a* for *h*-BC_4N-1 and BC_4N-1 at 9 GPa in Figure 4b suggest that the energy barrier is 0.24 eV at $c/a = 2.811$, less than 0.33 eV for the phase transition from 3*R*-graphite to diamond.[35] At $c/a = 2.811$, the enthalpy of *h*-BC_4N-1 is 161.509 eV, corresponding to the pressure of 14 GPa in Figure 4a. Therefore, the calculated dynamic pressure of the phase transition from *h*-BC_4N-1 to BC_4N-1 is 14 GPa, less than the used pressure of 20 GPa in synthesizing *c*-BC_4N.[3] When the pressure is applied to over 80 GPa, *h*-BC_4N-1 will transform completely to BC_4N-1, and this pressure value is the same as that for the phase transition predicted from 3*R*-graphite to diamond.[35]

In summary, we found that all five 3*C*-BC_4N configurations constructed with Ramsdell notation match the synthesized *c*-BC_4N in the XRD spectrum. However, BC_4N-1 has the lowest total energy and formation energy. In the view of energy, BC_4N-1 can be assigned as *c*-BC_4N. The calculation results indicate that *c*-BC_4N is a superhard material next to diamond. The dynamic pressure of the phase transition from *h*-BC_4N-1 to BC_4N-1 is only 14 GPa, less than the used pressure in synthesizing *c*-BC_4N. The simulated Raman spectrum for BC_4N-1 shows two strong peaks, one at about 1325 cm^{-1} from the contribution of the TO mode and the other at 1250 cm^{-1} from the contribution of the LO mode. This feature can be used as the criterion not only to determine the atomic arrangement of *c*-BC_4N but also to distinguish *c*-BC_4N from *c*-BC_2N.

Acknowledgment. This work was supported by NSFC (Grant Nos. 50472051, 50532020, and 10325417), by NBRPC (Grant Nos. 2005CB724400 and 2006CB921805), by PCSIRT (Grant No. IRT0650), and by the 111 project (Grant No. B07026).

References and Notes

(1) Liu, A. Y.; Cohen, M. L. *Science* **1989**, *245*, 841.
(2) Solozhenko, V. L.; Andrault, D.; Fiquet, G.; Mezouar, M.; Rubie, D. C. *Appl. Phys. Lett.* **2001**, *78*, 1385.
(3) Zhao, Y.; He, D. W.; Daemen, L. L.; Shen, T. D.; Schwarz, R. B.; Zhu, Y.; Bish, D. L.; Huang, J.; Zhang, J.; Shen, G.; Qian, J.; Zerda, T. W. *J. Mater. Res.* **2002**, *17*, 3139.
(4) Zhang, R. Q.; Chan, K. S.; Cheung, H. F.; Lee, S. T. *Appl. Phys. Lett.* **1999**, *75*, 2259.
(5) Mattesini, M.; Matar, S. F. *Int. J. Inorg. Mater.* **2001**, *3*, 943.
(6) Sun, H.; Jhi, S. H.; Roundy, D.; Cohen, M. L.; Louie, S. G. *Phys. Rev. B* **2001**, *64*, 094108.
(7) Kim, E.; Pang, T.; Utsumi, W.; Solozhenko, V. L.; Zhao, Y. S. *Phys. Rev. B* **2007**, *75*, 184115.
(8) Zhou, X. F.; Sun, J.; Fan, Y. X.; Chen, J.; Wang, H. T.; Guo1, X. J.; He, J. L.; Tian, Y. J. *Phys. Rev. B* **2007**, *76*, 100101(R).
(9) Pan, Z. C.; Sun, H.; Chen, C. F. *Phys. Rev. Lett.* **2007**, *98*, 135505.
(10) Chen, S. Y.; Gong, X. G.; Wei, S. H. *Phys. Rev. Lett.* **2007**, *98*, 015502.
(11) Guo, X. J.; Liu, Z. Y.; Luo, X. G.; Yu, D. L.; He, J. L.; Tian, Y. J.; Sun, J.; Wang, H. T. *Diamond Relat. Mater.* **2007**, *16*, 526.
(12) Hubble, H. W.; Kudryashov, I.; Solozhenko, V. L.; Zinin, P. V.; Sharma, S. K.; Ming, L. C. *J. Raman Spectrosc.* **2004**, *35*, 822.
(13) Zhou, X. F.; et al., unpublished.
(14) Ramsdell, L. S. *Am. Mineral.* **1947**, *32*, 64.
(15) Chen, S. Y.; Gong, X. G.; Wei, S. H. *Phys. Rev. B* **2008**, *77*, 9.
(16) Segall, M. D.; Lindan, P. J. D.; Probert, M. J.; Pickard, C. J.; Hasnip, P. J.; Clark, S. J.; Payne, M. C. *J. Phys.: Condens. Matter* **2002**, *14*, 2717.
(17) Ceperley, D. M.; Alder, B. J. *Phys. Rev. Lett.* **1980**, *45*, 566.
(18) Perdew, J. P.; Zunger, A. *Phys. Rev. B* **1981**, *23*, 5048.
(19) Lin, J. S.; Qteish, A.; Payne, M. C.; Heine, V. *Phys. Rev. B* **1993**, *47*, 4174.
(20) Monkhorst, H. J.; Pack, J. D. *Phys. Rev. B* **1976**, *13*, 5188.
(21) Fischer, T. H.; Almlof, J. *J. Phys. Chem.* **1992**, *96*, 9768.
(22) Roundy, D.; Krenn, C. R.; Cohen, M. L.; Morris, J. W. *Phys. Rev. Lett.* **1999**, *82*, 2713.
(23) Zhang, Y.; Sun, H.; Chen, C. F. *Phys. Rev. Lett.* **2004**, *93*, 195504.
(24) www.pwscf.org.
(25) Baroni, S.; de Gironcoli, S.; Dal Corso, A.; Giannozzi, P. *Rev. Mod. Phys.* **2001**, *73*, 515.
(26) Gonze, X.; Lee, C. *Phys. Rev. B* **1997**, *55*, 10355.
(27) Sun, J.; Zhou, X. F.; Chen, J.; Fan, Y. X.; Wang, H. T.; Guo, X. J.; He, J. L.; Tian, Y. J. *Phys. Rev. B* **2006**, *74*, 193101.
(28) Tateyama, Y.; Ogitsu, T.; Kusakabe, K.; Tsuneyuki, S.; Itoh, S. *Phys. Rev. B* **1997**, *55*, 10161.
(29) Nye, J. F. *Physical Properties of Crystals*; Oxford Science: Oxford, 1957.
(30) Born, M.; Huang, K. *Dynamical Theory of Crystal Lattices*; Oxford University Press: London, 1954.
(31) Pan, Z. C.; Sun, H.; Chen, C. F. *Phys. Rev. B* **2006**, *73*, 214111.
(32) Gao, F. M.; He, J. L.; Wu, E. D.; Liu, S. M.; Yu, D. L.; Li, D. C.; Zhang, S. Y.; Tian, Y. J. *Phys. Rev. Lett.* **2003**, *91*, 015502.
(33) He, J. L.; Wu, E. D.; Wang, H. T.; Liu, R. P.; Tian, Y. J. *Phys. Rev. Lett.* **2005**, *94*, 015504.
(34) Luo, X. G.; Liu, Z. Y.; Guo, X. J.; He, J. L.; Yu, D. L.; Tian, Y. J.; Sun, J.; Wang, H. T. *Chin. Phys. Lett.* **2006**, *23*, 2175.
(35) Fahy, S.; Louie, S. G.; Cohen, M. L. *Phys. Rev. B* **1986**, *34*, 1191.

JP801530Z